Experimental $M1$ transition rates in highly charged Kr ions

E. Träbert,[1,2,*] P. Beiersdorfer,[1] G. V. Brown,[1] H. Chen,[1] D. B. Thorn,[1] and E. Biémont[2]
[1]*Department of Physics and Advanced Technologies, Lawrence Livermore National Laboratory, Livermore, California 94550-9234*
[2]*IPNAS, Université de Liège, B-4000 Liège, Belgium*
(Received 17 February 2001; published 18 September 2001)

Atomic level lifetimes have been measured on magnetic dipole ($M1$) transitions in Si-like, P-like, Ar-like, K-like, and Ca-like ions of Kr, using an electron-beam ion trap in magnetic trapping mode. The lifetimes are compared to various predictions, including the results of different calculations. In Ar-like ions, magnetic quadrupole ($M2$) transitions have been identified as significant competing decay channels.

DOI: 10.1103/PhysRevA.64.042511 PACS number(s): 32.70.Cs, 32.30.Rj, 39.90.+d

I. INTRODUCTION

Because of the strong dependence of electrostatic term differences on the ionic charge, the prominent electric dipole ($E1$) transitions of highly charged ions lie in the vacuum-ultraviolet or x-ray ranges and feature upper-level lifetimes in the picosecond range. The fine structure intervals in moderately highly charged ions, however, are so much smaller that magnetic dipole ($M1$) and electric quadrupole ($E2$) transitions between fine-structure levels give rise to transitions in the visible spectral range. In the absence of competing decays, as is the case for the ground configuration of heavy ions, the typical level lifetimes are in the millisecond range. Such transitions are most useful for the diagnostic of laboratory and solar plasmas [1,2], because they relate to the lowest levels, and thus, are most easily excited. They permit the application of optical high-resolution techniques, and are low enough in transition rate so as to grant observations to larger optical depths than do $E1$ transitions. However, atomic measurements on the millisecond time scale require the ions to be trapped for the duration of the measurement. Various trapping schemes have been demonstrated, using the traditional ion traps, a heavy-ion storage ring, or an electron-beam ion trap [3].

Krypton is being discussed as a radiation blanket element for cooling the plasma edge and divertor regions in the next generation of fusion test devices. However, spectroscopic knowledge of the various charge states of krypton is sparse at best and nonexistent for many ions [4,5]. A recent development has been the use of an electron-beam ion trap for the spectroscopic study of highly charged ions, and the scope of the experiments has rapidly developed from survey spectra to fairly high resolution work [6–10]. In the course of these studies, it was found that the visible spectra of highly charged ions of many elements in the low-density environment inside the electron-beam ion trap are dominated by the so-called ''forbidden'' $M1$ transitions, many of which have not yet been classified. This classification is hampered by the steep scaling of the fine-structure intervals (and thus, the $M1$ transition wavelengths) with the nuclear charge Z and the ensuing lack of data to establish isoelectronic trends for inter- and extrapolation, as well as the persistent difficulties of theory in calculating fine-structure intervals to a useful precision. Because of the latter problem, calculations of the transition rates are even more uncertain (the $M1$ transition rates scale with the third power of Z), unless the calculated energy intervals can be adjusted semiempirically. Experimental information on the fine-structure intervals that make up the full transition energy of the $M1$ transitions so far has often been available only as small differences of large numbers (and thus, imprecisely), from extreme-ultraviolet spectra of tokamak plasmas [11].

The electron-beam ion trap has demonstrated its capability for precisely determining transition rates with atomic lifetime measurements in the millisecond and submillisecond ranges [12,13]. Closest among those studies to the present subject of visible transitions in highly charged Kr are the preceding studies on Ar, Kr, and Xe [6–8,14–16], and in particular on Kr XXIII, the spectrum of the Si-like ion Kr^{22+} [7,8,17]. In the latest of these investigations, lifetime measurements with a precision of up to 2% have been achieved at the Livermore electron-beam ion trap EBIT-II. All of those measurements concerned unbranched decays. In the ground configurations of many ions, however, branched decays are also common that may feature one optical decay branch that is accessible to efficient observation, while the total intensity is shared with other branches in less efficiently covered other ranges of the spectrum (such as the vacuum ultraviolet).

In the present paper, we report on lifetime measurements on low-lying levels of Si-like (no other experimental data beyond [8], but included for completeness), P-like, Ar-like, and K-like ions of krypton, as well as on a line that features similar properties, but remains as yet unidentified (we suggest identification with the Ca-like ion of Kr). We also present the results of different calculations, since such forbidden transition rates are calculated ''simply'' [18] only in principle, but not in practice, and because the published calculations do not cover all cases of present interest.

II. EXPERIMENT

The experiment was done on EBIT-II, the smaller one of the two electron-beam ion traps at the University of California Lawrence Livermore National Laboratory. The experimental technique has been detailed before [8,16], so that a

*Permanent address: Fakultät für Physik und Astronomie, Ruhr-Universität Bochum, D-44780 Bochum, Germany; email address: traebert@ep3.ruhr-uni-bochum.de

 ©2001 The American Physical Society

few general remarks should be sufficient here. The electron beam in an electron-beam ion trap serves to excite atoms and ions, provides space-charge compensation for the ion cloud produced and contributes to radial trapping by an attractive potential. For this, the electron beam is being compressed and guided by a strong magnetic field ($B=3$ T), and it runs along the axis of symmetry of a series of cylindrical drift tubes. The latter are staggered in positive potential, so that ions can be trapped axially. In the present paper, krypton was bled into the trap under ultrahigh vacuum conditions (the pressure inside EBIT-II is of the order 10^{-10} mbar and less). The gas plume intersects the electron beam inside the trap volume, where then successive ionization (and some recombination) take place until a charge-state balance is reached. The ionization ends at a stage where the electron-beam energy can no more overcome the ionization potential. This implies that by a variation of the electron-beam energy, the charge-state balance can be adjusted and a maximum charge state be predetermined.

For the lifetime measurement, the electron-beam ion trap was run in a cyclic mode. For example, an electron beam of about 1.2 keV energy was used to produce an appropriate charge-state distribution that included Kr^{21+} among the highest charge states reached. Then the electron beam was switched off while the optical emission was monitored. After a period corresponding to about ten times the expected atomic lifetime, the remaining ions were expelled from the trap (by lowering one of the end drift tube voltages) and the cycle started anew.

Even after the electron beam that usually provides an attractive potential and space-charge compensation is switched off, the ion cloud remains trapped in a Penning ion trap formed by the strong magnetic field and the 250 V difference drift tube voltages, in the so-called magnetic trapping mode of the electron-beam ion trap [19]. Upon switching, the ion cloud expands somewhat, but then remains stationary. Light emission from the ion cloud is collected by an optical system with a 10 cm diameter, *f*/4 lens system and transported to a low-noise photomultiplier tube (Hamamatsu R2557, 13 mm diameter, head-on design). A free-running 100 kHz frequency generator provides time markers for a fast scaler. The arrival of a photon signal triggers the digitization of the time value in the scaler [20], and the number of time markers is stored in the event mode system as a time stamp for the event. In the present paper, the ion trap was cycled every about 200 to 250 ms, with about equal time spent on ion production and excitation on one hand and the electron-beam off for the observation of decay curves on the other. At the electron-beam energies used here (0.65 to 1.4 keV), the switching of the electron-beam acceleration voltage and of the electron-beam current required about 30 μs, which is much faster than the atomic lifetimes studied (of 800 μs and more).

III. CALCULATIONS

For their extensive (though incomplete) tabulation of forbidden transitions in the $n=2$ and 3 shells (up to $3p$), Kaufman and Sugar [21] employed Dirac-Fock and Cowan code calculations to derive missing line positions and transition rates. The latter code was also used by Crespo López-Urrutia *et al.* [6] in their search for identifications of unknown lines, including estimates of transition rates. However, little detail on the calculations is given in either of those studies. We therefore supplemented the published calculations by our own. These were of two types, the Hartree-Fock approach with relativistic corrections (HFR method) using the Cowan code [22], and a multiconfiguration Dirac-Fock (MCDF) code as originally presented by Grant and McKenzie and coworkers [23,24]. The first technique is very useful for obtaining reliable level-structure information after semiempirical adjustment of certain parameters. According to a well-established semiempirical procedure [22], the electrostatic, $F^k\,(a,b)$, $G^k\,(a,b)$, the spin-orbit, ζ_{nl}, and the configuration interaction integrals, $R^k\,(a,b;c,d)$, were first calculated *ab initio* using the HFR method and were then, in a second step, considered as free parameters and adjusted in order to fit the calculated eigenvalues of the Hamiltonian to the observed energy levels. Some correlation effects involving distant configurations, not explicitly introduced in the physical model, were implicitly considered by scaling down the Slater integrals. The second, fully relativistic, MCDF method was applied for obtaining transition rates of higher-multipole-order transitions.

IV. DATA AND DISCUSSION

In previous work of the Livermore EBIT group, a number of forbidden transitions in multiply to highly charged ions of Kr have been recognized in survey spectra of the visible range. Very few of such lines were known before [21], and a few more of these could be classified, varying the electron-beam energy in the electron-beam ion trap in order to determine their excitation thresholds [6]. This investigation has since been continued with better spectral resolution [10]. Lines were associated with K- to Si-like ions of krypton. One line at 545.3 nm, by its appearance clearly in the same class as the identified $M1$ transitions, has not yet been identified. As its production threshold is lower than that of the line associated with the K-like ion, it is bound to result from one of the next isoelectronic sequences with a $3d^k$ configuration. However, these ions differ so little in ionization potential that an unequivocal identification of the charge state was not feasible.

Some of the optical decay curves (samples are shown in Figs. 1 and 2) showed first a steep drop, as is encountered often in optical lifetime measurements using an electron-beam ion trap. This drop originates from a combination of ending the prompt emission by ending the excitation, changes in the brightness of the electron gun filament, and some initial ion loss from the observation zone. (Occasionally, one finds trap parameters that result in practically no sudden drop, and thus permit to exploit the excited ions best.) Next followed the curve part of interest with the lifetime component of principal interest. In curves of a high signal-to-background ratio, often a third, much slower, component (associated with charge-exchange processes, see below) appears that then dips into the detector-dark rate domi-

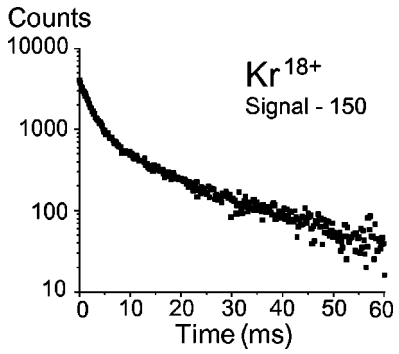

FIG. 1. Photon signal (logarithmic scale) obtained with Kr XIX at a wavelength of 402.7 nm (decay of the $3s^2 3p^5 3d\ ^3P_2$ level), after the electron beam in the electron-beam ion trap is switched off (magnetic trapping mode). A background of 150 counts per channel has been subtracted from the data.

nated background. The characteristic time of the principal component was determined from up to four measurements per line, under different conditions (variation of excitation energy, cycle time, and trap depth).

The apparent optical lifetime results from a combination of radiative decays (this transition rate is wanted) and ion losses from the sample under study (by collisional diffusion across the magnetic field, evaporation from the stored ion cloud along the magnetic field, and overcoming the confining electrical potential walls, or charge-exchange (CX) collisions, most likely with the neutral rest gas). No appropriate measurements of the storage time constant for Kr ions in the magnetic trapping mode (electron beam off) are available, because the ions of present interest have no x-ray decay channels that could be monitored best for such CX processes. We therefore can only estimate the associated uncertainties of the atomic lifetime results. With lighter ions (Ar, K) than krypton, ion storage lifetimes of order 250 to 500 ms were measured in experiments close in time and to other running conditions of the present experiments [25]. However, it is well known that heavy ions are confined more effectively than light ions while the electron-beam ion trap is

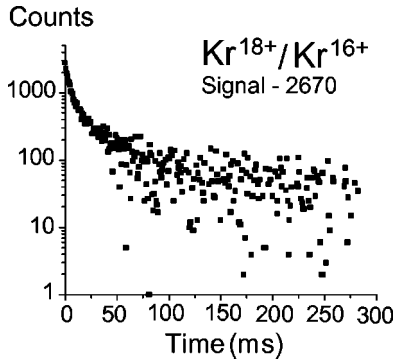

FIG. 2. Photon signal (logarithmic scale) obtained with lines from both Kr XIX (decay of the $3s^2 3p^5 3d\ ^3F_2$ level) and an unidentified ion of Kr (probably Kr^{16+} seen through a filter centered at 570 nm with 50 nm bandpass. Out of the full data, only the part after switching off the electron beam is shown. A background of 2670 counts per channel has been subtracted from the data.

in the electronic trapping mode (electron beam on). Also, the charge-state distribution is wider with heavy ions than with light ions. This increases the chance that gains and losses of ions of the species of interest that are due to CX processes with other ions largely cancel for charge states near the middle of the distribution. The present decay curves do not yield clear information in this respect. However, assuming ion loss rates as quoted above, we expect systematic shifts of order 1% for lifetimes of about 2 to 5 ms, and of 10% for lifetimes of about 20 to 50 ms, with the apparent lifetimes always being shorter than the true atomic lifetimes. Such a correction is negligible (in comparison to the statistical uncertainty) for the short lifetimes measured here, but is quite notable for the long ones. We present lifetime results based on the raw data and corrected for a probable ion storage lifetime of 300 ms, assuming half of the associated loss rate as the likely error of the correction.

We aimed at lifetime measurements of all candidate lines. The strongest line in the visible spectrum of krypton in an electron beam ion trap, the $3s^2 3p^2\ ^3P_1$-$^3P_2$ transition in Si-like Kr XXIII, has been presented separately as it showed peculiarities when studied with high-spectral resolution [8]. Being such a prominent spectral feature, this line was an obvious choice for trying out the lifetime measurement capabilities of electron-beam ion traps. However, as might be expected with a different measurement technique, the first attempts [7,17] for different reasons turned out less than satisfactory, before in a third step, a clean measurement was achieved [8]. A calculation (see below) has been performed that perfectly corroborates our latest (and probably last) experimental lifetime result [8].

Of the remaining lines, six appeared strongly in the survey spectra. However, the combination of our photomultiplier tube (with a nominal working range 300–630 nm) and of the available filters restricted the coverage somewhat. For example, a (nominally) 315 nm filter with a 5 nm bandpass did not let pass any signal of the 313.4 nm transition (S-like Kr XXI $3s^2 3p^4\ ^3P_2$-$^3P_1$). In another case, our filters permitted only the simultaneous observation of two lines, not a recording of individual decay curve data. This, of course, adds some ambiguity to the interpretation of those data. The basic measurement parameters of all our cases covered are listed in Table I. In the following, the observations and interpretations are listed by isoelectronic sequence. The lifetime results are summarized and compared to theory in Table II.

A. Kr XXIII

According to the NIST compilation of spectroscopic reference data,[1] the five levels of the $3s^2 3p^2$ configuration have been experimentally determined, the $^1S_0$ level, however, being affected by a larger uncertainty. We have performed a HFR calculation for Kr XXIII using the configuration set $3s^2 3p^2 + 3p^4 + 3s 3p^2 3d + 3s^2 3d^2 + 3p^2 3d^2 + 3s 3d^3 + 3d^4$. The calculated eigenvalues were adjusted to the NIST levels.

[1]Accessible at the Web address: http://physics.nist.gov/PhysRefData

TABLE I. Ionic systems and measurement parameters. The investigation on Kr XXIII has been reported elsewhere [8].

Ion	Spectrum	Sequence	Production threshold (eV) [40]	Electron-beam energy (eV) used in this work	Filter mean wavelength and bandpass (nm)
Kr^{17+}	Kr XVIII	K	588	650–750	640/10
Kr^{18+}	Kr XIX	Ar	604	750–1150	415/45
Kr^{18+}	Kr XIX	Ar	604	750–950	570/50
Kr^{21+}	KrXXII	P	886	1350	345/10
Kr^{22+}	Kr XXIII	Si	935	1000–1400	385/5
$Kr^{??+}$	Kr (Unidentified)		≈500 (exp.)	750–950	570/50

Adopting also a scaling factor of 0.95 for the parameters not fitted (except for the spin-orbit integrals which were left unchanged), the following results were deduced for the transitions depopulating the $^3P_2$ level: $^3P_0$-$^3P_2$ $(E2)$: $A=4.594\ s^{-1}$, $^3P_1$-$^3P_2$ $(E2)$: $A=6.882\times10^{-3}\ s^{-1}$, $^3P_1$-$^3P_2$ $(M1)$: $A=143.5\ s^{-1}$. The lifetime value calculated for the $^3P_2$ level is $\tau=6.75$ ms that agrees quite well with the latest experimental result [8]. This calculation is also an improvement over the ''old'' HFR calculation published by Biémont and Bromage [26] using a similar technique but a smaller configuration basis set that leads to a value of $\tau=6.46$ ms.

B. Kr XXII

In the *P*-like ion Kr^{21+}, the $^2D^o_{5/2}$ level of the $3s^2\ 3p^3$ ground configuration decays predominantly to the $^4S^o_{3/2}$ ground level (at a wavelength of 91.2 nm [21], a wavelength

TABLE II. Comparison of predicted and measured upper-level lifetimes τ for the krypton ions studied. The wavelengths given are rounded literature values (see text).

Spectrum	Transition	Wavelength (nm)	Lifetime (ms) experiment	Theory
Kr XVIII	$3s^2 3p^6 3d\ ^2D_{5/2} \rightarrow {}^2D^o_{3/2}$	636.9	22.7±1.0 (This work)	24.6 [38]
				24.0 [38] [a]
				23.8 [39]
				24 [6]
				23.8 [c]
Kr XIX	$3s^2 3p^5 3d\ ^3P^o_2 \rightarrow {}^3P^o_1$	402.7	2.20±0.2 (This work)	⩽5 [6] [b]
				1.52 [d]
Kr XIX	$3s^2 3p^5 3d\ ^3F^o_2 \rightarrow {}^3F^o_3$	579.3	4.2±0.5 (This work)	⩽10 [6] [b]
				4.20 [d]
Kr XXII	$3s^2 3p^3\ ^2D^o_{5/2} \rightarrow {}^2D^o_{3/2}$	344.6	0.80±0.03 (This work)	0.73 [27]
				0.72 [28]
				0.78 [21]
				0.78 [c]
				0.81 [d]
Kr XXIII	$3s^2 3p^2\ ^3P_2 \rightarrow {}^3P_1$	384.2	6.82±0.1 [8]	6.46 [26]
				6.78 [26] [a]
				5.83 [41]
				6.69 [41] [a]
				6.85 [21]
				6.75 [c]
Kr (Unidentified)		545.3	≈4.2 or 40±5 (This work) (not individually observed)	
suggested identification				
Kr XVII	$3p^6 3d^2\ ^3P_2 \rightarrow {}^1D_2$	546 [c]		8.6 [c]
				10.2 [42]

[a]Theoretical results afterwards adjusted for the experimental transition energy.
[b]Branched decay, reference quotes calculation for observed branch only.
[c]This work, HFR calculation (see text).
[d]This work, MCDF calculation (see text).

not presently accessible to us), while a 14% branch fraction decays to the $^2D^o_{3/2}$ level. This branch has been predicted to occur at a wavelength of 344.6 nm [21], and it has been observed at 346.47 nm [7,14]. Kaufman and Sugar [21] predict a total decay rate of 1282 s^{-1}, or a level lifetime of 0.78 ms, which renders this the shortest-lived of the ones of present interest. This value has been confirmed by our data (0.80 ± 0.03 ms). The ion storage-time correction is negligible for such a short atomic lifetime.

According to the NIST compilation (see above), 5 levels of the $3s^2 3p^3$ configuration are known experimentally, but only with large uncertainties. Fixing the scaling factor of the Slater integrals in our calculations at 0.95, we varied the spin-orbit integral ζ_{3p} of the $3s^2 3p^3$ configuration in order to reproduce adequately the observed wavelengths. Using the configurations $3s^2 3p^3 + 3p^5 + 3s3p^3 3d + 3s^2 3p 3d^2 + 3p^3 3d^2 + 3s3p3d^3 + 3p3d^4$, we found $\zeta_{3p} = 60750$ cm^{-1} as the best choice. The lifetime value of the $^2D^o_{5/2}$ level was then deduced by combining the four transitions that originate from that level, i.e., $^4S^o_{3/2}$-$^2D^o_{5/2}$: $A_{M1} = 1098\, s^{-1}$, $^2D^o_{3/2}$-$^2D^o_{5/2}$: $A_{M1} = 172.7$ s^{-1}, $^4S^o_{3/2}$-$^2D^o_{5/2}$: $A_{E2} = 9.207$ s^{-1}, $^2D^o_{3/2}$-$^2D^o_{5/2}$: $A_{E2} = 8.012 \times 10^{-3}$ s^{-1}. This leads to a lifetime value of $\tau = 0.78$ ms, in very good agreement with our experimental result. Earlier predictions, from calculations with smaller configuration sets [27,28], were lower by about 10%, which is outside our error estimate. Adopting the MCDF method, but with a smaller set of nonrelativistic configurations (i.e., $3s^2 3p^3 + 3s3p^3 3d + 3p^3 3d^2 + 3p^5$), the calculated lifetime result is $\tau = 0.81$ ms, a result that is in excellent agreement both with experiment and with the HFR result. We note that Mendoza and Zeippen [29] have also treated P-like ions, but not as high in charge as Kr^{21+}.

C. Kr XIX

The $3p^5 3d$ level structure in Ar-like ions of the iron group has been studied theoretically by Wagner and House [30] who also applied semiempirical corrections after some forbidden lines had been identified as arising from such ions [31]. Of the twelve $3p^5 3d$ levels (Fig. 3), only the three levels with $J=1$ can decay to the $3p^6\ ^1S_0$ ground state via electric dipole ($E1$) transitions. These three $J=1$ levels have lifetimes that differ by several orders of magnitude. The fastest decay ($^1P^o_1$ level) is easily observed in various plasmas [32], whereas the next slower one ($^3D^o_1$) is often quenched collisionally (except in low-density tokamak plasmas [32] or in the beam-foil light source), while the decay of the longest-lived of these levels ($^3P^o_1$) remains elusive so far [33]. A similar situation is found in Kr-like ions, and there even a trend reversal leading to a lifetime increase with higher ionic charge has been found in beam-foil observations of the $4p^5 4d\ ^3D^o_1$ level decay [34].

All other $3p^5 3d$ levels in Ar-like ions decay only via higher-multipole order transitions (like $M1$ or $M2$) to each other or the ground state, if at all. Crespo López-Urrutia *et al.* [6] include estimates of the $M1$ transition rates (that is, of the directly observed transitions) with their identifications

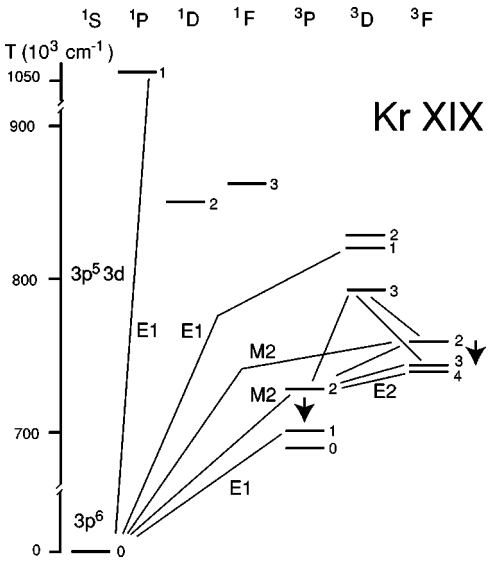

FIG. 3. Level scheme of the $3s^2 3p^5 3d$ levels in the Ar-like ion Kr^{18+} (Kr XIX). The level energies are from our calculations, and thus, are approximate only. Arrows mark the $M1$ transitions observed here. The other connecting lines indicate important decay branches that involve the levels of present interest directly (competing $M2$ decay) or as major direct and indirect cascades from levels with millisecond and longer lifetimes.

of the $3p^5 3d\ ^3P^o_1$-$^3P^o_2$ and $^3F^o_3$-$^3F^o_2$ lines. In both cases, the present lifetime measurements yield total decay rates that are higher than those transition rates by about a factor of two to three. Such a difference might indicate that other decay channels are present, and the $M2$ decays of the $J=2$ levels to the ground state are obvious candidates for those. However, no calculations of these branches seem to have been published. In order to alleviate this lack of comparison data, new HFR and MCDF calculations have been undertaken. The full set of calculations and results will be presented elsewhere [35]. Here, we will discuss only that part of the paper that relates to the immediate context of our experimental study.

In addition to the intraconfiguration deexcitation by $M1$ and $E2$ transitions, the $^3P^o_2$ and $^3F^o_2$ levels of the $3s^2 3p^5 3d$ configuration can decay to the ground $3p^6\ ^1S_0$ level through $M2$ channels. These $M2$ contributions cannot be obtained directly with the aforementioned Cowan code. For that reason, we have estimated their contribution with a fully relativistic *ab initio* approach (MCDF method, Grant code [23,24]). Using a set of three nonrelativistic configurations, i.e., $3s^2 3p^5 3d + 3s3p^6 3d^2 + 3p^6 3d^3$, which are expected to catch the largest part of the correlation effects, we have verified that the $M2$ contributions were of the same order of magnitude as the $M1$ ones. More precisely, the numerical results were as follows: $^1S_0$-$^3P^o_2$ $A_{M2} = 444.1$ s^{-1}, $^1S_0$-$^3F^o_2$ $A_{M2} = 132.8$ s^{-1}, $^3P^o_1$-$^3P^o_2$ $A_{M1} = 213.5$ s^{-1}, $^3F^o_3$-$^3F^o_2$ $A_{M1} = 85.90$ s^{-1}, $^3P^o_1$-$^3F^o_2$ $A_{M1} = 0.653$ s^{-1}, and $^3P^o_2$-$^3F^o_2$ $A_{M1} = 18.81$ s^{-1}. The $E2$ contributions were found to be substantially smaller, the largest ones being $^3P^o_0$-$^3F^o_2$ $A_{E2} = 0.329$ s^{-1}, $^3P^o_1$-$^3F^o_2$ $A_{E2} = 0.776$ s^{-1}, and $^3P^o_2$-$^3F^o_2$ A_{E2}

$=6.37\times10^{-2}$ s^{-1} and, consequently, play a negligible role in the present context.

From the above calculations, lifetime values of τ ($^3P_2^o$) $=1.52$ ms and τ ($^3F_2^o$)$=4.20$ ms were deduced. The second result is in excellent agreement with the experiment (see below) while the first one is notably lower than the experimental finding of 2.0 to 2.4 ms. This might indicate that the calculated transition probability of the $^1S_0$-$^3P_2^o$ $M2$ transition is too large, possibly caused by the neglect of other configurations within the $n=3$ complex due to computer capability limits. This point was checked by a HFR calculation with a larger configuration set within the $n=3$ complex than in the MCDF calculation above. However, when adding the $3s3p^33d^4+3s3p3d^6+3p^53d^3+3p3d^7$ configurations, the transition rate of the $M1$ $^3P_1$-$^3P_2$ transition was modified only in a minor way, to A (HFR)$=214.6$ s^{-1}. It was also verified that adding the $n=4$ excitation has a negligible effect on the final results. This stability of the theoretical result suggests that the experimental lifetime value for the $^3P_2$ may be affected by other factors, for example, by cascade repopulation (see discussion below).

Our only filter that permitted to see the 402.7-nm line of Ar-like Kr XIX ($3p^53d\,^3P_1^o$-$^3P_2^o$) was centered at 415 nm and had a bandpass of 45 nm. In order to ascertain that this filter blocked out the strong 384-nm line of Kr XXIII, decay curves were recorded at various electron-beam energies down to below the excitation threshold of the Si-like ion. No variation of the apparent lifetime was found, and thus, apparently, no contamination was suffered. However, if contamination was present, the ratio of the two lifetime components would be about three to four. It would be difficult to properly disentangle such a case.

Another such disentanglement problem arises from the term structure of Kr XIX itself. Assuming that the decay curve (Fig. 1) is dominated by a single component, a lifetime result of 2.1 ± 0.1 ms will be obtained. However, the $3p^53d\,^3P_2^o$ level lies below the $J=2$, 3, 4 levels of the other terms of the same configuration, and hence, cascade repopulation from those levels has to be considered. This problem is also hinted at by the result of our calculation that yields a lifetime prediction of 1.5 ms for the $^3P_2^o$ level. Fitting an additional major decay component to the same decay curve data, a primary lifetime of about 2.0 ms was obtained, with the additional component showing a time constant of about 9 ms. However, the statistical reliability of the data is not high enough to determine whether this is, in fact, a single dominant component or whether this is representing several cascades. Anyway, several cascades with time constants within a factor of three of each other, have been tackled in beam-foil spectroscopy for decades, and it is known that only correlated cascade analyses can provide reliable lifetime data in such cases. As it happens, one of the cascades, a 20% decay branch of the $3p^53d\,^3F_2^o$ level, has been measured in our experiment (see below), but its lifetime of 4.2 ms appears not to be the only one contributing to the $3p^53d\,^3P_2^o$ level decay curve. With the variety of options of how to interpret the decay curve data, we present a lifetime result of 2.2 ± 0.2 ms that includes both major variants. In such a complex cascade situation, alas, an overall systematic error of order 30% (towards a too-long apparent lifetime) is conceivable (but not verifiable with our present means). Therefore,the calculated lifetime of 1.5 ms should not be considered as being contradicted by the present evaluational results.

For lack of more specific filters, another line in Ar-like Kr XIX ($[3p^53d\,^3F_3^o$-$^3F_2^o]$, $\lambda=579.3$ nm [6]) and an unidentified forbidden line at 545.3 nm were observed jointly through a 570-nm, 50-nm bandpass filter (Fig. 2). Here, a very long observation time was needed to ensure a statistical reliability that would permit the analysis of a multicomponent superposition of decay curves. The data curves clearly yielded two decay components that are different by about a factor of ten. The individual fit results for the decay components, however, varied by about 10%. It was expected that at the lower electron-beam energy, the unidentified line would dominate, and vice versa. The experiment, however, showed only a little, inconclusive change of the ratio of the two decay amplitudes. We assume that the shorter-lived component belongs to the transition of interest in Kr XIX, because a previous calculation [6] that included a single decay branch only must provide an upper bound to the true lifetime. Our calculations indeed corroborated this assumption, with a calculated level lifetime of 4.2 ms that is in perfect agreement with our experimental finding.

For now, however, it remains an open question whether the measured lifetime value belongs to the Kr XIX $^3F_2$ level exclusively or whether the unidentified line has an approximately similar time constant (which would also explain why no significant variation occurred when the excitation conditions were changed). After all, in the nonrelativistic limit, $M1$ transition rates depend only on Racah geometry factors and the transition energy [18], and with transitions of similar wavelengths, an incidental coincidence of the geometry factors, and thus, of the transition probabilities might happen. The slower decay component of about 36 ms (raw data) requires the largest correction for the assumed ion loss rate and thus would correspond to a level lifetime of order 40 ms in a collision-free environment.

The situation is further complicated by the pattern of dominant transitions in the level scheme of Kr XIX (see Fig. 3), involving several levels with (calculated) millisecond lifetimes. The $^3D_3$ level decays predominantly to the $^3P_2$ level, but also to $^3F_2$ and $^3F_3$. The $^3F_2$ level decays to $^3P_2$ (the aforementioned cascade), but also to $^3F_3$, a level with a two-second lifetime that in turn then repopulates the $^3P_2$ level. Thus, some delays appear in the cascade chain, but also the millisecond lifetime component that is due to the $^3D_3$ level. From our HFR and MCDF calculations, the lifetime of this level is predicted in the 1.45 to 8 ms range. A problem of the latter calculation is the large difference (a factor of 4 to 6) between the transition rate results of our exploratory calculations in Coulomb and Babushkin gauges, of which the latter (related to the length gauge in nonrelativistic calculations) is generally assumed to be the more reliable one. Interestingly, the lowest level of the ^3F term, $^3F_4$, is predicted to have a lifetime of more than 30 000 s (taking $M1$, $E2$, and $M2$ decay channels into account). This would be enormous for a level some 80 eV above the ground state,

and it might call for more detailed calculations that include even higher multipole-order radiation ($M4$ decay to the ground state?). Of course, in a real-world environment, such a long natural lifetime would appear shortened by collisions and electromagnetic fields.

D. Kr XVIII

The 636.9-nm line of K-like Kr XVIII was barely seen through a 640-nm (bandpass 10 nm) filter, because of the poor efficiency of the detector in this range. Also, the filament of the electron gun in EBIT-II had to be reduced in temperature (and thus, the electron-beam current) in order to reduce the red stray light reaching the detector through the filter. Nevertheless, within about 24 h, sufficiently meaningful decay data were accumulated that yielded a lifetime of 22 ms. Adding to this an estimate of the ion storage time and its associated uncertainty, a lifetime of (22.7 ± 1.0) ms was found.

For K-like Kr XVIII, Yang and Li [36] have calculated the $3d$ fine-structure interval (in reasonable agreement with an experimental value obtained from wave-number differences of allowed transitions [11,37]) and oscillator strengths of $3d$-$4f$ transitions, but not the probability of the forbidden transition of present interest. However, the wanted theory data are available from Ali and Kim [38] and from Biémont and Hansen [39], and we add a calculation to these, too. According to the aforementioned NIST compilation, the level $3p^6 3d\,^2D_{5/2}$ of the ground configuration of Kr XVIII is well established ($E = 15\,694$ cm^{-1}). By considering, inside the $n=3$ Layzer complex, the set of configurations $3s^2 3p^6 3d + 3s^2 3p^4 3d^3 + 3s^2 3d^7 + 3s 3p^6 3d^2 + 3p^6 3d^3 + 3p^2 3d^7 + 3d^9$, and by using average energy and spin-orbit parameters deduced by a least-squares adjustment of the levels, we have obtained for $3p^6 3d\,^2D_{5/2}$ a theoretical lifetime $\tau = 23.87$ ms. Some correlation effects involving distant configurations, not explicitly introduced in the physical model, were implicitly considered by scaling down the Slater integrals. The weighted $M1$ transition probability corresponding to the above lifetime result is $A = 41.90$ s^{-1}, the $E2$ contribution being negligible at $A \simeq 2.60 \times 10^{-4}$ s^{-1}. The scaling factors of the integrals, not adjusted in the calculation, were arbitrarily fixed at 0.95 (except for the spin-orbit integrals that were kept at their *ab initio* values), but it was verified that the calculated lifetime is not dependent upon the choice of the scaling factors. The calculated lifetime is near the upper limit of the present measurement and its uncertainty ($\tau = 22.7 \pm 1.0$ ms). It is also very close to the semiempirical result deduced previously by a similar HFR method by Biémont and Hansen [39], i.e., $\tau = 23.85$ ms.

E. Kr XVII-XIV

For Kr ions in lower-charge states (say, the Ca through V isoelectronic sequences), such as for the one indicated by the excitation function for the aforementioned unknown line, the NIST database holds no entries on levels or transition rates, and earlier searches based on Cowan code calculations failed to suggest a suitable identification. The main indicator to follow is the wavelength, and thus, the transition energy. The observed time constant (of either 4 ms or of 40 ms, see discussion above) may relate either to the upper level of the transition or to a cascading level, possibly a high-J level of the same term, that feeds it. One possible identification from our calculations is that with the $3p^6 3d^2\,^1D_2$-$^3P_2$ transition in Ca-like Kr XVII. The predicted wavelength (546 nm) is almost coincident with the observation (545.3 nm), and the upper-level lifetime, predicted as 8.6 ms, is of the right order of magnitude. Given the limited accuracy of the fine-structure energy calculation, the wavelength coincidence may be fortuitous and is not sufficient as a proof of identity. However, several other transitions in the same configuration are predicted to give rise to lines in the near vacuum ultraviolet, which can eventually be probed spectroscopically and will then help to establish the level structure in more detail.

The same holds for the vast number of levels in the $3d^3$ ground configuration of (Sc-like) Kr XVI and in the $3d^4$ ground configuration of (Ti-like) Kr XV, and so on. Our calculations indicate level lifetimes that are typically in the range between one millisecond and one second, and transition wavelengths that range from the infrared to the near vacuum ultraviolet. While some of the lines by virtue of their predicted wavelength (and compatible upper-level lifetime) might be alternative candidates for the unknown line discussed above, such identifications would then require the appearance of (admittedly weaker) other decay branches from the same upper level, or of certain other lines from the same ion. There is not enough evidence in the spectra for either of those, which leaves the identification suggested above as the presently best choice. The first decay component then represents a blend of two decays with not very different upper-level lifetimes, while the second, slow decay component may represent a superposition of cascade contributions; we have not been able to identify a fitting individual level of this lifetime in a likely decay chain.

The vast number of transitions in the ground configurations of $3d$ shell ions, however, also implies that most of the individual lines will be weak. Therefore, these lines are not prominent, but must appear as part of the spectral background in the prism spectrometer survey spectra recorded on the electron-beam ion trap [6]. Future EBIT work at higher spectral resolution, and at rather low electron-beam energies, can be expected to reveal a wealth of information on those configurations.

V. CONCLUSIONS

In all cases studied in the present paper (and including Kr XXIII [8]), there is satisfactory agreement of measurement and calculation, if the latter is adjusted to the experimental term differences. This, however, is a problem for the user of forbidden lines, as the experimental data base is grossly incomplete and insufficient for reliable isoelectronic analyses. The confirmation of suggested line identifications threshold testing using the electron-beam energy in EBIT and now the lifetime determination should help to improve predictions for

neighboring elements, so that eventually, a more complete data set can be derived for its many uses in terrestrial and extraterrestrial plasma diagnostics.

In Ar-like Kr XIX, two levels have been identified that decay about equally by $M1$ and $M2$ branches in the visible and vacuum ultraviolet (VUV) ranges. Such line pairs may be of interest in plasma diagnostics, as the calculations of both branches can be done about equally well, and thus, the prediction of the branching ratio can be assumed to be similarly reliable. This is in contrast to the frequently used pairs of in-shell and intershell decays of which the latter is much more reliably calculated than the former. Measurements and calculations need to be combined to make certain that all decay branches of a given level are being considered. After all, it is a feature that in laboratory experiments on low-lying excited levels $M1$ and $E2$ transitions compete with $M2$ transitions and possibly even higher-order multipole decays.

Note added in proof. The 40 ms second lifetime component in the decay curve of the Kr XVII line (Table II) has meanwhile been recognized as an artifact related to the temporal thermal response of the electron gun.

ACKNOWLEDGMENTS

We are happy to acknowledge the dedicated technical support by Ed Magee and Phil D'Antonio, and the loan of the photomultiplier by Joe Holder. The work at the University of California Lawrence Livermore National Laboratory was performed under the auspices of the Department of Energy under Contract No. W-7405-Eng-48 and supported by the Chemical Sciences, Geosciences and Biosciences Division of the Office of Basic Energy Sciences, Office of Science, U.S. Department of Energy. E.T. acknowledges travel support from the German Research Association (DFG) and support by FNRS (Belgium).

[1] B. Edlén, Z. Astrophys. **22**, 30 (1942).
[2] B. Edlén, Phys. Scr. T **8**, 5 (1984).
[3] E. Träbert, Phys. Scr. **61**, 257 (2000).
[4] J. Sugar and A. Musgrove, J. Phys. Chem. Ref. Data **20**, 859 (1985).
[5] T. Shirai, K. Okazaki, and J. Sugar, J. Phys. Chem. Ref. Data **24**, 1577 (1995).
[6] J.R. Crespo López-Urrutia, P. Beiersdorfer, K. Widmann, and V. Decaux, Phys. Scr. T **80**, 448 (1999).
[7] E. Träbert, P. Beiersdorfer, S.B. Utter, and J.R. Crespo López-Urrutia, Phys. Scr. **58**, 599 (1998).
[8] E. Tráabert, S.B. Utter, and P. Beiersdorfer, Phys. Lett. A **272**, 86 (2000).
[9] J.R. Crespo López-Urrutia, P. Beiersdorfer, K. Widmann, and V. Decaux (unpublished).
[10] H. Chen, P. Beiersdorfer, C.L. Harris, E. Trabert, S.B. Utter, and K.L. Wong, Phys. Scr. T **92**, 284 (2001).
[11] J.F. Wyart and TFR group, Phys. Scr. **31**, 539 (1985).
[12] J.R. Crespo López-Urrutia, P. Beiersdorfer, D.W. Savin, and K. Widmann, Phys. Rev. A **58**, 238 (1998).
[13] E. Träbert, P. Beiersdorfer, G.V. Brown, A.J. Smith, M.F. Gu, and D.W. Savin, Phys. Rev. A **60**, 2034 (1999).
[14] F.G. Serpa, E.W. Bell, E.S. Meyers, J.D. Gillaspy, and J.R. Roberts, Phys. Rev. A **55**, 1832 (1997).
[15] F.G. Serpa, C.A. Morgan, E.S. Meyer, J.D. Gillaspy, E. Träbert, D.A. Church, and E. Takács, Phys. Rev. A **55**, 4196 (1997).
[16] E. Träbert, P. Beiersdorfer, S.B. Utter, G.V. Brown, H. Chen, C.L. Harris, P.A. Neill, D.W. Savin, and A.J. Smith, Astrophys. J. **541**, 506 (2000).
[17] F.G. Serpa, J.D. Gillaspy, and E. Träbert, J. Phys. B **31**, 3345 (1998).
[18] L.J. Curtis, Phys. Scr. T **8**, 77 (1984).
[19] P. Beiersdorfer, L. Schweikhard, J. Crespo López-Urrutia, and K. Widmann, Rev. Sci. Instrum. **67**, 3818 (1996).
[20] P. Beiersdorfer, G.V. Brown, L. Hildebrandt, K.L. Wong, and R. Ali, Rev. Sci. Instrum. **72**, 508 (2001) (in press).
[21] V. Kaufman and J. Sugar, J. Phys. Chem. Ref. Data **15**, 321 (1986).
[22] R.D. Cowan, *The Theory of Atomic Structure and Spectra* (University of California Press, Berkeley, CA, 1981).
[23] I.P. Grant, B.J. McKenzie, P.H. Norrington, D.F. Mayers, and N.C. Pyper, Comput. Phys. Commun. **21**, 207 (1980).
[24] B.J. McKenzie, I.P. Grant, and P.H. Norrington, Comput. Phys. Commun. **21**, 233 (1980).
[25] E. Träbert, P. Beiersdorfer, G.V. Brown, H. Chen, E.H. Pinnington, and D.B. Thorn, Phys. Rev. A. **64**, 034501 (2001).
[26] E. Biémont and G.E. Bromage, Mon. Not. R. Astron. Soc. **205**, 1085 (1983).
[27] J. Sugar and V. Kaufman, J. Opt. Soc. Am. B **1**, 218 (1984).
[28] E. Biémont and J.E. Hansen, Phys. Scr. **31**, 509 (1985).
[29] C. Mendoza and C.J. Zeippen, Mon. Not. R. Astron. Soc. **198**, 127 (1982).
[30] W.J. Wagner and L.L. House, Astrophys. J. **155**, 677 (1969).
[31] W.J. Wagner and L.L. House, Astrophys. J. **166**, 683 (1971).
[32] J. Sugar, V. Kaufman, and W.L. Rowan, J. Opt. Soc. Am. B **4**, 1927 (1987).
[33] E. Träbert, M. Brandt, J. Doerfert, J. Granzow, P.H. Heckmann, J. Meurisch, I. Martinson, R. Hutton, and R. Myrnäs, Phys. Scr. **48**, 580 (1993).
[34] E. Träbert, Phys. Lett. A **167**, 69 (1992).
[35] E. Biémont (unpublished).
[36] L. Yang and J.M. Li, J. Phys. B **25**, 649 (1992).
[37] V. Kaufman, J. Sugar, and W.L. Rowan, J. Opt. Soc. Am. B **6**, 142 (1989).
[38] M.A. Ali and Y.-K. Kim, Phys. Rev. A **38**, 3992 (1988).
[39] E. Biémont and J.E. Hansen, Phys. Scr. **39**, 308 (1989).
[40] R.L. Kelly, J. Phys. Chem. Ref. Data Suppl. **16**, 1 (1987).
[41] K.-N. Huang, At. Data Nucl. Data Tables **32**, 503 (1985).
[42] U.I. Safronova, W.R. Johnson, D. Kato, and S. Ohtani, Phys. Rev. A **63**, 032518 (2001).